

**Pre- and post-punching failure performances of flat slab-column joints with drop panels and shear studs**

Author

Jiao, Ziyang, Li, Yi, Guan, Hong, Diao, Mengzhu, Yang, Zhi, Wang, Junkun, Li, Yichen

Published

2022

Journal Title

Engineering Failure Analysis

Version

Accepted Manuscript (AM)

DOI

[10.1016/j.engfailanal.2022.106604](https://doi.org/10.1016/j.engfailanal.2022.106604)

Rights statement

© 2022 Elsevier. Licensed under the Creative Commons Attribution-NonCommercial-NoDerivatives 4.0 International Licence (<http://creativecommons.org/licenses/by-nc-nd/4.0/>) which permits unrestricted, non-commercial use, distribution and reproduction in any medium, providing that the work is properly cited.

Downloaded from

<http://hdl.handle.net/10072/418550>

Griffith Research Online

<https://research-repository.griffith.edu.au>

# 1 **Pre- and post-punching failure performances of flat slab-column** 2 **joints with drop panels and shear studs**

3  
4 Ziyang Jiao<sup>a,b</sup>, Yi Li<sup>a,\*</sup>, Hong Guan<sup>b,\*</sup>, Zhi Yang<sup>a,b</sup>, Mengzhu Diao<sup>b</sup>, Yichen Li<sup>a</sup>, Junkun Wang<sup>a</sup>

5 <sup>a</sup> Beijing Key Laboratory of Earthquake Engineering and Structural Retrofit, Beijing University  
6 of Technology, Beijing 100124, China.

7 <sup>b</sup> School of Engineering and Built Environment, Griffith University, Gold Coast Campus,  
8 Queensland 4222, Australia.

9 **Abstract:** To investigate the pre- and post-punching failure performances of flat slab-column  
10 joints with drop panels and shear studs, static loading tests were conducted on three joint  
11 specimens subjected to in-plane restraints. The pre- and post-punching failure modes and load  
12 capacities of the joints were analysed. The test identified successive punching failures at two  
13 critical regions (column perimeter and slab-drop panel interface) in all three joints. Compared  
14 with the specimen with a drop panel only, installing shear studs within the drop panels  
15 contributed to improving the punching shear strength. Although the post-punching capacity  
16 was not significantly improved, utilisation of shear studs effectively increased the ductility of  
17 the joints, rendering the punching failure around the column area more ductile. Punching shear  
18 strength validation against the international design codes reveals that they are conservative for  
19 the specimen with a drop panel only but overestimated for specimens with drop panels and  
20 shear studs.

21 **Keywords:** slab-column joint, drop panel, shear stud, pre- and post-punching failure mode,

---

\* Corresponding authors, Emails: yili@bjut.edu.cn (Y. Li), h.guan@griffith.edu.au (H. Guan)

22 pre- and post-punching strength

23

## 24 **1. Introduction**

25 Reinforced concrete (RC) flat plate system is a slab and column structure without the use of  
26 beams. Flat slab structures are flat plates with drop panels and column capitals at the slab-  
27 column joints. They represent a very simple form of construction in which slabs are supported  
28 directly on columns [1]. These types of structures are increasingly used in high-rise residential  
29 and office buildings and car parks because of their pleasing architectural style, easy  
30 construction formwork and low construction cost. However, compared with frame structures,  
31 slab-column joints in flat plate structures are prone to brittle punching failure, resulting in a  
32 low deformation capacity. Due to their beamless structural style, the surrounding slabs provide  
33 alternative load paths (ALP) after the initial punching failure taking place at one or more slab-  
34 column joints. Consequently, gravity loads on the slabs are redistributed to the adjacent intact  
35 joints through ALP, escalating the risk of subsequent punching failure there. Failure  
36 propagation may finally trigger a progressive collapse of such a structure, either completely or  
37 a large part of it [2]. Progressive collapse events of RC flat plate structures are catastrophic and  
38 always accompanied by a tremendous loss of life and property. For instance, the collapse events  
39 of Sampoong Department Store in South Korea in 1995 [3] and the Surfside condominium  
40 building in the U.S. in 2021 [4] caused more than five hundred and nearly one hundred deaths,  
41 respectively. However, international design codes for preventing and mitigating progressive  
42 collapse of various configurations of flat plate structures are still inadequate [5-6]. It is  
43 therefore vitally important to investigate the progressive collapse behaviour of these types of

44 structural systems, in particular, the ultimate strength and deformation capacity of the critical  
45 slab-column joints.

46

47 Progressive collapse is a mechanical behaviour of the structural system at the large deformation  
48 stage, in which slab-column joints typically undergo three deformation stages: flexural stage  
49 and punching failure stage in small deformations, and post-punching stage in large  
50 deformations. Specifically, slab-column joints transfer the load from slab to column, exhibiting  
51 an initial flexural behaviour provided by the combined effect of the concrete and reinforcing  
52 bars (rebars) in the flexural stage, a subsequent tensile membrane action provided by the rebars  
53 passing through the column in the post-punching stage [7]. Currently, most published studies  
54 related to the mechanical behaviour of slab-column joints mainly focus on their performance  
55 in the small deformation stage under gravity and seismic loading scenarios. For instance, some  
56 investigations [8-10] only highlighted flexural and punching failure mechanisms, whereas the  
57 suspension mechanism in the post-punching stage was ignored [11-14]. However, in-depth  
58 studies on progressive collapse require more attention on the entire deformation stages,  
59 particularly, the post-punching stage. All of these stages have significant impact on the collapse  
60 mechanism of the flat plate structural systems. In addition, the applied boundary conditions for  
61 the slab-column joints in the existing studies also restrict the scope of the research findings. In  
62 some experimental work [14-15], the boundary of the tested joints was set as simply supported.  
63 This does not truly reflect the continuity conditions in a real flat plate structure where joints  
64 are confined by the surrounding slabs. Therefore, certain degrees of in-plane restraints should  
65 be applied to the boundary of isolated slab-column joints. Simplification of the boundary

66 conditions may cause underestimation of the punching strengths and prevent the suspension  
67 mechanism to be activated in the post-punching stage [16-20]. The latter can yield considerable  
68 post-punching resistance provided by through-column rebars. Therefore, thorough  
69 investigations on both pre- and post-punching failure performances of the slab-column joints  
70 with in-plane restraints are in an essential need for a comprehensive understanding of the  
71 progressive collapse behaviour of flat plate systems.

72

73 To improve the ductility and punching shear resistance of slab-column joints, a large number  
74 of strengthening methods have been proposed and tested by researchers, such as using ultra-  
75 high-performance concrete or ultra-high-performance fiber reinforced concrete in place of a  
76 part of normal concrete [21-22], applying prestressing tendons [23], adding shear  
77 reinforcement together with the rebar mesh, etc. [12-13]. In addition to all these, drop panels  
78 have also been popularly used in flat slab structures as a feasible strengthening method owing  
79 to their notable advantages in cost-saving and strength improvement [24-26]. Note that for a  
80 flat plate slab-column joint, punching shear failure occurs in the vicinity of the critical  
81 perimeter cross-section around the column. For a slab-column joint with a drop panel in a flat  
82 slab structure, on the other hand, an additional punching failure section close to the slab-drop  
83 panel interface is also of critical concern. In order to fully utilise the material strength, the  
84 design punching shear strength at the column critical perimeter is normally required to be  
85 greater than that at the drop panel interface. The mechanical behaviour of slab-column joints  
86 with drop panels becomes more complicated because two potential punching and post-  
87 punching failures require attention at the flexural, punching and suspension stages. Relevant

88 research on both punching and post-punching failure mechanisms of slab-column joints with  
89 drop panels is still scarce. Experimentally, Qian and Li [27] tested six one-third-scaled flat slab  
90 substructures with or without drop panels under corner column removal scenarios to evaluate  
91 the effectiveness of the drop panels in resisting progressive collapse. Test results revealed that  
92 specimens with drop panels acquired a higher punching shear resistance, initial stiffness and  
93 energy dissipation capacity. However, punching failure was not observed in specimens with  
94 drop panels. Further, Qian and Li [28] compared the performance of two  $2 \times 2$  bays flat slab  
95 substructures with and without drop panels under a middle column removal scenario and it was  
96 found that the drop panels can effectively prevent the generation and propagation of punching  
97 failure at the slab-column joints. Numerically, Weng et al. [29] investigated the load  
98 redistribution capacity of flat slab substructures in resisting progressive collapse. Their  
99 proposed models were validated by experimental test results [28], and based on which the  
100 parametric studies consisting of varying boundary conditions, integrity reinforcement ratios,  
101 slab thicknesses and upper floor effects were performed to explore their influences on the  
102 progressive collapse resistance. Both experimentally and numerically, Qian et al. [30] studied  
103 the dynamic response of flat slab structures with drop panels subject to a single interior column  
104 removal and both interior and edge column removal scenarios. These previous studies have  
105 successfully assessed the progressive collapse resistance of flat slab structural systems under  
106 normal design load and the effectiveness of drop panels in improving load-resistant capacity.  
107 Limited studies, however, have addressed the post-punching mechanism subsequent to two  
108 punching failures at both critical column perimeter and slab-drop panel interface regions,  
109 especially the latter.

110

111 In recent years, some progressive collapse accidents of flat slab structures with drop panels  
112 have been reported in China because of overloading during the construction phase. In these  
113 accidents, overloading only triggered punching shear failure at a few individual joints, yet the  
114 internal load redistribution led to more widespread subsequent failures. In addition to drop  
115 panels, shear studs are also recommended by the international codes as an effective  
116 strengthening method to improve the punching shear strength of slab-column joints. The ease  
117 of installation and anchorage allows them to work effectively with the drop panels to further  
118 improve the ductility and punching shear resistance of the slab-column joints. Langohr et al.  
119 [31] and Seible et al. [32] carried out a series of experimental tests to investigate the  
120 enhancement of punching shear strength and ductility of slab column joints under different  
121 shear stud arrangements. It was found that the best enhancement results were achieved when  
122 the shear studs were arranged in orthogonal and radial patterns. Indeed, shear studs are often  
123 arranged in an orthogonal pattern or a radial pattern in practice. The former is broadly applied  
124 in North America whereas the latter is preferred in Europe. Birkle and Dilger [33] specifically  
125 investigated the effect of two shear stud placements (orthogonal or radial) on the punching  
126 shear resistance of slab-column joints for varied situations (i.e. spacing and coverage of shear  
127 studs). Their test results showed that the slab-column joints with two placements resulted in  
128 the same punching shear strength under the same situation. The orthogonal placement was  
129 recommended due to its simplicity in installation. On the contrary, Broms [34], and Dam and  
130 Wight [35] reached opposite conclusions. In their studies, shear studs in the radial pattern  
131 performed better than the orthogonal pattern in improving punching shear resistance and

132 ductility of the slab-column joints. To this end, mixed findings are resulted from the existing  
133 studies as which arrangement performs better. In addition, these experimental studies did not  
134 examine the post-punching performance and appropriate in-plane restraints were not  
135 considered. Therefore, investigations on the load-resistant and deformation capacities of slab-  
136 column joints with drop panels and shear studs during the entire deformation stage, especially  
137 in the post-punching stage, are still insufficient to date.

138

139 To fill this research gap, an experimental study on three scaled-down flat slab-column joint  
140 specimens with proper in-plane restraints was conducted. One specimen had a drop panel only,  
141 and two other specimens had shear studs, arranged in either the orthogonal or the radial pattern.  
142 The load-displacement responses, failure modes, and material strain growth patterns were  
143 discussed in detail. Moreover, the punching shear capacities of the three specimens were  
144 predicted by the American (ACI 318) and European (EC 2) building codes [24-25]. The  
145 underlying reasons causing the discrepancies between the experimental and code predicted  
146 results were also discussed.

147

## 148 **2. The experimental program**

149 The prototype structure is a three-storey RC flat slab underground car park structure with drop  
150 panels which was designed according to the Chinese code [26]. Improper stacking of backfill  
151 during its construction resulted in overloading and caused initial column damage at a single  
152 slab-column joint, which in turn triggered progressive collapse of a large part of the car park  
153 area. Typical planar layout of a standard story in the prototype structure can be simplified as

154 shown in Fig. 1, in which the span length ( $l$ ) is 8100mm, column size is 600mm  $\times$  600mm, slab  
 155 thickness is 350mm and the concrete cover is 25mm. The dimension of the drop panel is  
 156 4050mm  $\times$  4050mm with a linear variation in depth (maximum depth of 450mm at the column  
 157 edge and minimum depth of 250mm at the drop panel edge as presented in Fig. 1). The tested  
 158 specimens were based on the initially damaged joint in the prototype and were designed and  
 159 cast with a part of surrounding slabs. As a result, appropriate boundary conditions can be  
 160 applied to the specimens. Based on the theoretical calculation [1], the contra-flexural lines in  
 161 the slab are located  $0.56l$  away from the centre of the initially damaged column. For ease of  
 162 transportation and fixation in the laboratory, the boundary of the specimens was chosen at a  
 163 distance of  $0.5l$  extending two directions from the column centrelines, approximately matching  
 164 the contra-flexural lines [11-13].  
 165

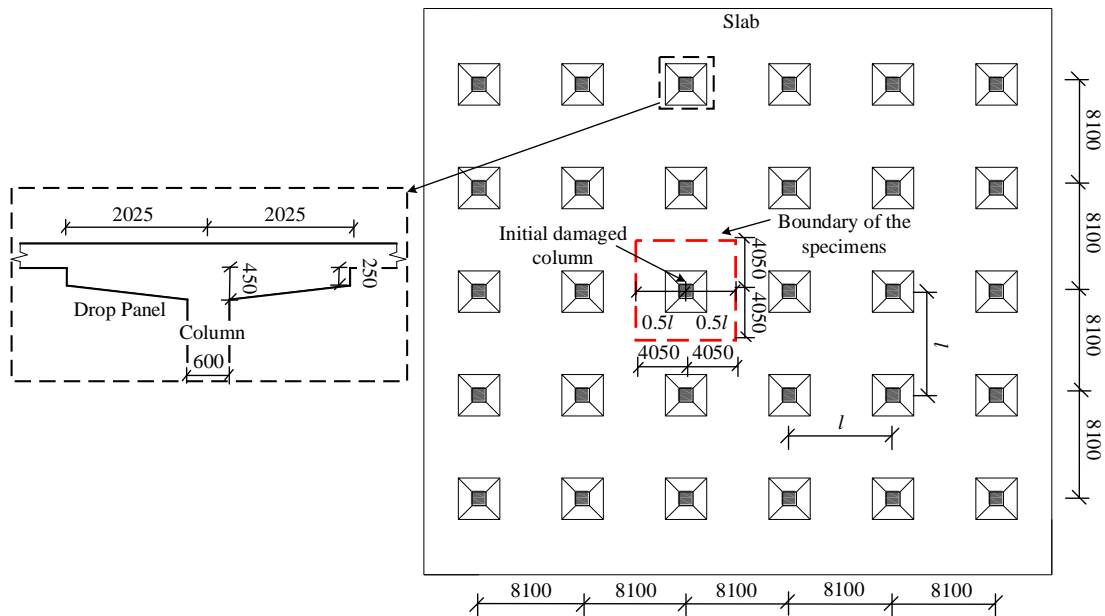


Fig.1. Plan view of the simplified prototype structure (unit: mm).

166

167 A total of three specimens were tested and reported. The control specimen (Specimen DP) was  
 168 directly extracted from the prototype, that is, keeping the reinforcement type, reinforcement  
 169 ratio and concrete grade constant with the prototype but scaled down in geometry with a ratio  
 170 of 1:4. To the approximate whole numbers, the slab dimension of DP was of 2000mm×  
 171 2000mm, the slab thickness was 90mm, the column dimension was 150mm×150mm and the  
 172 concrete cover was 6mm. The drop panel in DP had a dimension of 1000mm×1000mm, and  
 173 the maximum and minimum depths were 110mm and 60mm, respectively (Fig. 2). The flexural  
 174 reinforcement (FR) at the slab top consisted of 8mm and 10mm HRB400 bars, the integrity  
 175 reinforcement (IR) at the slab bottom and the reinforcement in drop panels were both made up  
 176 of 8mm HRB400 bars. More details about the rebar distributions and reinforcement ratios can  
 177 be found in Table 1 and Fig. 2.

178

179

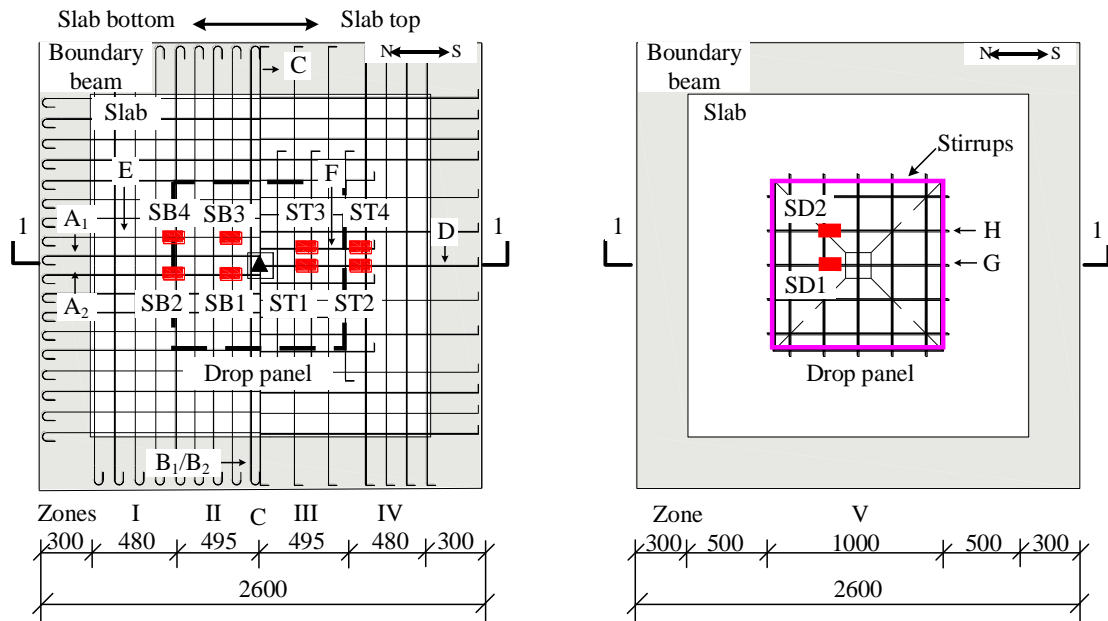
Table 1. Reinforcement configuration details in specimens.

Location		Distribution	Reinforcement ratio	
Slab	Bottom (IR)	Zone I	R8@120 <sup>a</sup>	0.62%
		Zone II	R8@110 <sup>a</sup>	0.6%
	Top (FR)	Zone III	R8@200 & R10@200 <sup>a</sup>	0.86%
		Zone IV	R8@120 <sup>a</sup>	0.48%
Drop panel	Zone V	R8@200 & 1R8 <sup>b</sup>	0.28%	

180 Note: “R” represents hot-rolled ribbed bars; the superscript “a” donates reinforcement being extended to the  
 181 boundary beams; “b” means reinforcement serving as stirrup.

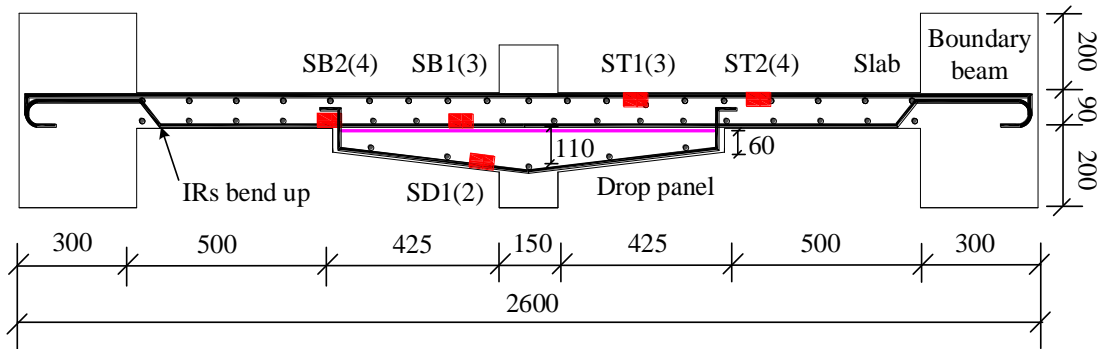
182

183



(a) Slab reinforcement details

(b) Drop panel reinforcement details



(c) 1-1 sectional view

Note: ■, strain gauges, which were installed on the same half of the slab. ▲, linear variable differential transformer. Rebars A<sub>1</sub>, A<sub>2</sub>, D, E, F, G, H were in outer layers, rebars B<sub>1</sub>, B<sub>2</sub>, C were in inner layers.

Fig.2. Reinforcement details (unit: mm).

184

185 To investigate the effectiveness of the slab-column joints with drop panels strengthened by  
 186 shear studs, specimens SSR and SSO were designed and constructed by adding shear studs in  
 187 DP [33-35]. SSR had a single row of shear studs arranged along the orthogonal and diagonal  
 188 directions forming a radial pattern, whereas SSO had double rows of shear studs arranged along

189 the orthogonal directions only in an orthogonal pattern (Figs. 3a, b and c). Shear studs in both  
 190 specimens were installed covering the two critical regions, namely the column perimeter and  
 191 the slab-drop panel interface. They were designed in accordance with the Chinese code [36].  
 192 The shear studs were in a double-headed style comprising three components: (1) the upper  
 193 continuous steel plate on top of (2) a series of vertical steel bars, and (3) the small steel plates  
 194 at the base of each steel bar. The vertical bars were made of 8mm HPB300 steel and was welded  
 195 to the upper and lower steel plates (Fig. 3d). The size, steel grade and quantity of shear studs  
 196 were the same for both SSR and SSO specimens. Their geometric dimensions and  
 197 reinforcement details were kept consistent with DP. The material properties of the three  
 198 specimens are summarised in Table. 2.

199

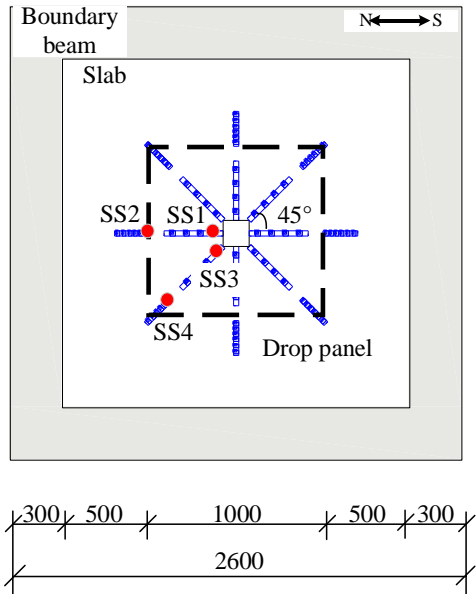
200

Table 2. Material properties of tests specimens.

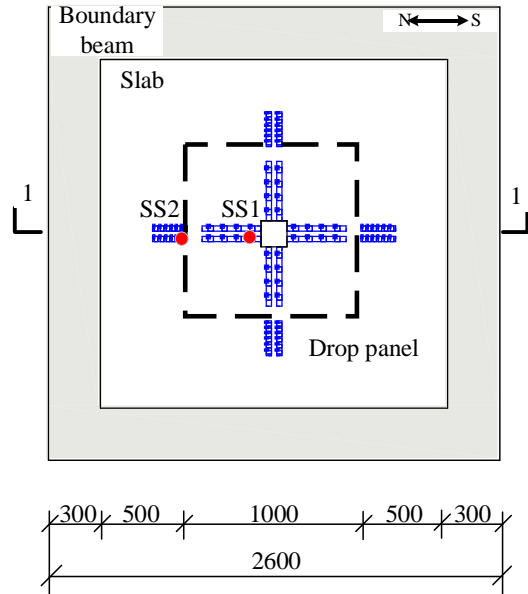
Reinforcement type	Reinforcement			Concrete	
	Yield strength (MPa)	Ultimate strength (MPa)	Ratio of elongation (%)	Elastic modulus (GPa)	Cubic compressive strength of concrete (MPa)
P8	347	487	14		
R8	404	617	11	205	33
R10	416	336	30		

201 Note: “P” and “R” represent the hot-rolled plain bars and hot-rolled ribbed bars, respectively.

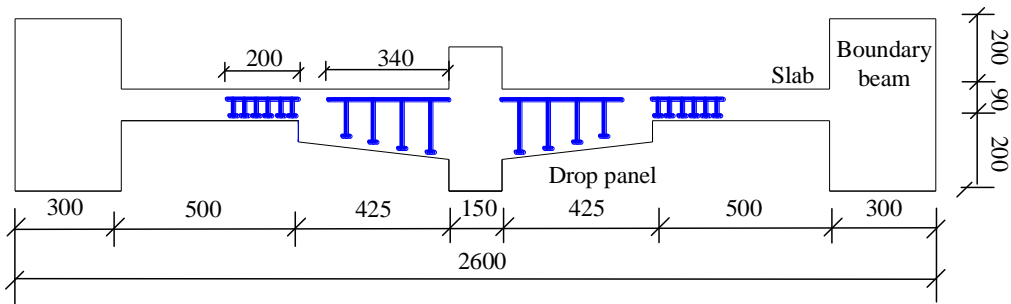
202



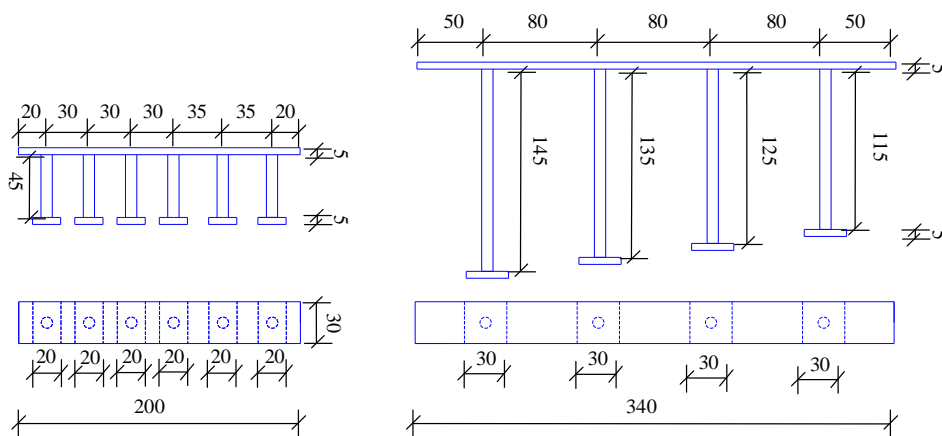
(a) Shear stud in radial pattern



(b) Shear stud in orthogonal pattern



(c) 1-1 sectional view



(c) 1-1 sectional view

Note: ● , strain gauges, which were installed at the middle of shear studs.

Fig. 3. Two arrangements of shear studs and shear stud details.

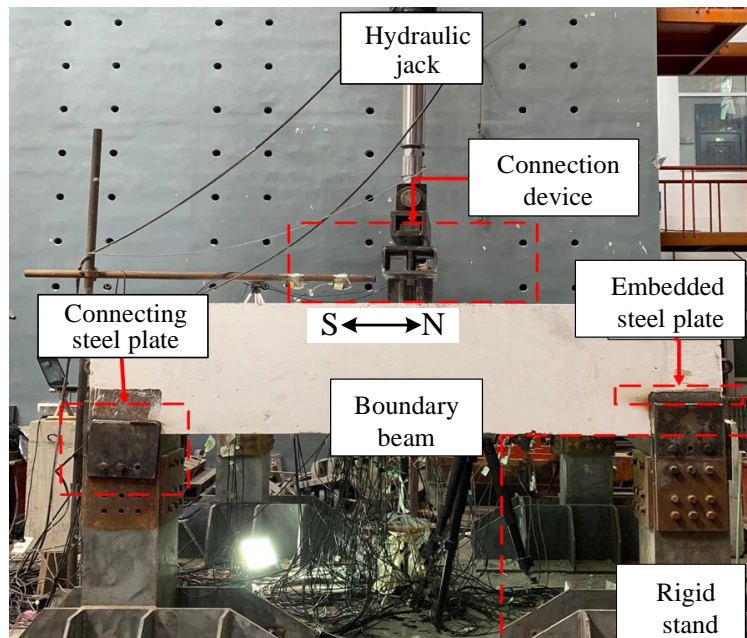
203 To simulate the boundary constraints on the isolated slab-column joints imposed by the  
204 surrounding slab in a real structure, rigid boundary beams were mounted at the edges of the  
205 slab. Apart from providing in-plane restraints to the specimens, the boundary beams also  
206 provided enough anchorage to the extended FR and IR in the slab, enabling specimens to  
207 exhibit a suspension mechanism after punching failure as in a real structure. As the interface  
208 between the slab and the boundary beams is approximately aligned with the contra-flexural  
209 lines in the prototype structure, the rotation and translation of the slab should be fully restrained  
210 by the surrounding slabs under the small deformation stage, whereas the slab should only be  
211 horizontally restrained in the large deformation stage. To achieve such restraint conditions  
212 during the entire deformation stage, the IR was bent up at the slab-boundary beam interface  
213 and further extended into the boundary beams (see Fig. 2c). Because no rebars were placed at  
214 the bottom of the interface to resist tensile moment, the concrete there would damage shortly  
215 after the specimens come into the large deformation stage, the rotational restraint from the  
216 boundary beams was thus released. The maximum horizontal translation of the boundary beams  
217 of the three specimens was measured to be 5.18mm, which was less than the deflection limit  
218 of  $1/200l_b$  ( $l_b$  is the boundary beam length) as specified in the Chinese code [26], confirming  
219 that the boundary beam remained in an elastic state and was able to provide sufficient in-plane  
220 restraint and anchorage.

221

222 The test setup is presented in Fig. 4. The specimens were supported on four rigid strands by  
223 welding and bolting to the embedded steel plates and connection steel plates on the boundary  
224 beams. The rigid strands were fixed on the strong floor in the laboratory to provide sufficient

225 rigidity to the specimens during the entire loading stage. Four 25mm-diameter steel rods were  
226 pre-installed in the column which were used to connect the hydraulic jack and column through  
227 a connection device. The hydraulic jack had enough stroke to supply monotonic upward  
228 loading until the specimens underwent large deformations until finally exhausted all their load  
229 resistant capacities. In this experimental program, a quasi-static loading scheme was adopted.  
230 The loading speed was controlled by the column displacement. The reaction force was  
231 monitored by the force transducer installed in the hydraulic jack. Linear variable displacement  
232 transducers were placed at the center of the column to measure its vertical displacement. In  
233 addition, strain growth in the rebars and shear studs at the critical locations (SBs, STs and SDs  
234 in Fig. 2 for bottom, top and drop panel rebars, respectively and SSs in Fig. 3 for shear studs)  
235 were recorded by strain gauges.

236



237

238

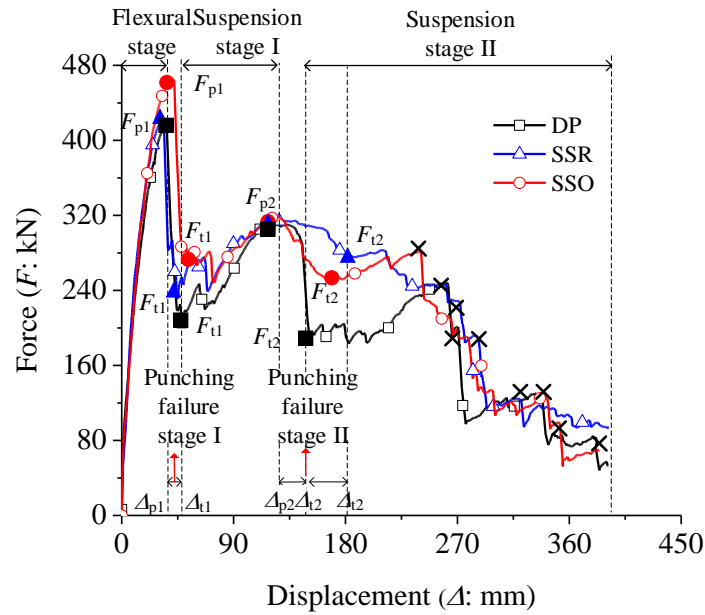
Fig. 4. Test setup.

239

### 240 **3. Experimental observations and results**

241 The load ( $F$ )-displacement ( $\Delta$ ) curves of the three test specimens are illustrated in Fig. 5, where  
242  $F$  and  $\Delta$  represent the reaction force and the vertical displacement of the column, respectively.  
243 Based on experimental observations and measurements, the deformation process of the three  
244 specimens can be divided into five stages: flexural stage, punching failure stages I and II, and  
245 suspension stages I and II. The flexural stage is defined as the deformation stage from the  
246 beginning of the test until the first punching failure occurs, during which the applied load on  
247 the specimens was resisted by the slab in flexural behaviour. The punching failure stage refers  
248 to the short period after punching failures took place and before re-ascending of  $F$ . The  
249 punching failure stages I and II are matched with two punching failures observed at the slab-  
250 drop panel interface regions and the column perimeter regions, respectively. The suspension  
251 stages I and II denote the stages after the punching shear failure, in which the load-resisting  
252 mechanism is governed by the rebars going through column and other rebars crossing the  
253 punching cracks. Furthermore, the terminologies and key points on the load-displacement  
254 curves are described. The peak loads  $F$ s attained before the two punching shear failures  
255 occurred are, namely, the first punching load ( $F_{p1}$ ), or the punching strength, at the slab-drop  
256 panel interface and the second punching load ( $F_{p2}$ ) at the column perimeter, which is also  
257 regarded as the post-punching strength. They are represented by two key points ( $F_{p1}$ ,  $\Delta_{p1}$ ) and  
258 ( $F_{p2}$ ,  $\Delta_{p2}$ ). The load drops after punching failures and before load re-ascending are identified as  
259 the residual strengths, and the corresponding key points are ( $F_{t1}$ ,  $\Delta_{t1}$ ) and ( $F_{t2}$ ,  $\Delta_{t2}$ ).

260



261

262 Note: × denotes rebar rupture.

263

Fig. 5. Load-displacement curves for DP, SSR and SSO.

264

### 265 3.1 Specimen DP

266 In the flexural stage, diagonal cracks initially appeared from the corners of the slab top at

267  $\Delta=5\text{mm}$ . When  $\Delta=9\text{mm}$  and  $31\text{mm}$ , two square-shaped crack rings were developed on and

268 beyond the slab-drop panel interface on the slab top, the side lengths of the rings were  $1000\text{mm}$

269 and  $1400\text{mm}$ , respectively (Fig. 6(a)). The specimen DP reached its punching shear strength

270 (i.e.  $F_{p1}=415\text{kN}$ ) at a displacement of  $36\text{mm}$ . The first punching failure was in a cone shape,

271 expanded from the slab-drop panel interface at the bottom to the larger crack ring on the slab

272 top. This first punching failure caused a sudden loss in  $F$  (i.e. from  $F_{p1}=415\text{kN}$  to  $F_{t1}=219\text{kN}$ ).

273 Thereafter, the specimen deformed into the suspension stage I during which  $F$  rose again. As

274 the punching cone gradually separated from the slab, the surrounding concrete was severely

275 damaged and unable to provide further resistance. In consequence, the specimen could only

276 transfer the tensile force by the rebars going through column and other rebars crossing the

277 punching cracks. At  $\Delta = 132\text{mm}$ , the second punching failure occurred near the column  
 278 perimeter, which also exhibited a distinct brittle mode of failure causing another sudden loss  
 279 in  $F$  (i.e. from  $F_{p2}=310\text{kN}$  to  $F_{t2}=186\text{kN}$ ). As the loading proceeded, the column was almost  
 280 detached from the specimen with the only connection being provided by the through-column  
 281 rebars. Due to the small quantity of through-column rebars, the load  $F$  could not regain the  
 282 same magnitude as  $F_{p2}$  at the second punching failure. Therefore, the post-punching strength  
 283 of DP was achieved when the second punching failure occurred. In suspension stage II,  
 284 through-column FR bars (rebars C and D in Fig. 2) were pulled out from the concrete. Through-  
 285 column rebars  $A_1$  and  $A_2$ ,  $B_1$  and  $B_2$ , C, D (Fig. 2) were ruptured in sequence. Thereafter, the  
 286 specimen exhausted all the load-resisting capacity. Typical test phenomena with their  
 287 corresponding  $F$ s and  $\Delta$ s are tabulated in Table 3. The crack patterns and final failure mode  
 288 are presented in Fig. 6(a) and Fig. 7(a). Note that the cracks on the slab bottom surface were  
 289 mainly in circumferential forms around the column, the slab-drop panel interface as well as  
 290 along the slab edges.

291

292

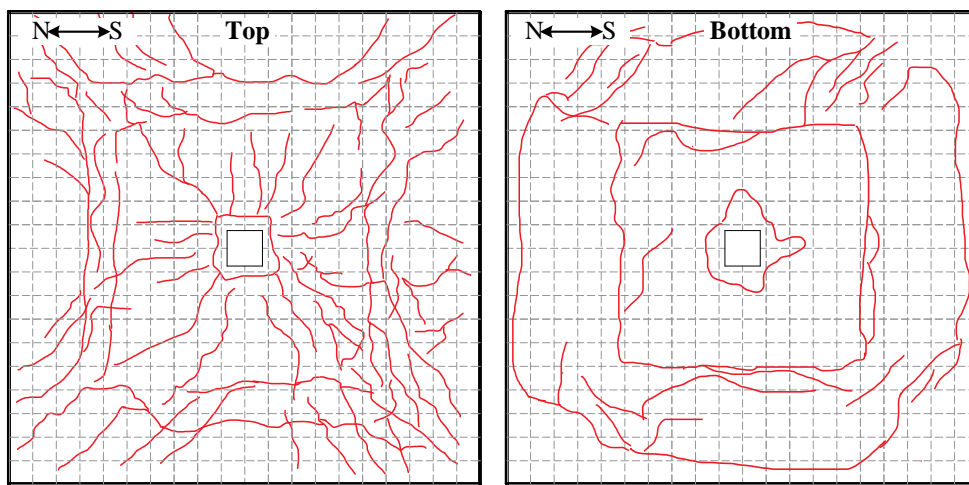
Table 3. Typical phenomena during the tests

Typical phenomenon	DP		SSR		SSO	
	$F$ (kN)	$\Delta$ (mm)	$F$ (kN)	$\Delta$ (mm)	$F$ (kN)	$\Delta$ (mm)
Initial cracks	137	5	193	7	194	8
Punching crack rings	406	31	367	21	360	20
First punching failure	415	36	425	32	465	41

Residual strength after first punching failure	219	45	283	37	281	48
Second punching failure	310	132	315	124	319	123
Residual strength after second punching failure	186	151	275	169	251	187
Rebars rapture	248	260	246	259	280	240

293 Note: “ $F$ ” and “ $\Delta$ ” represent reaction force and column vertical displacement, respectively.

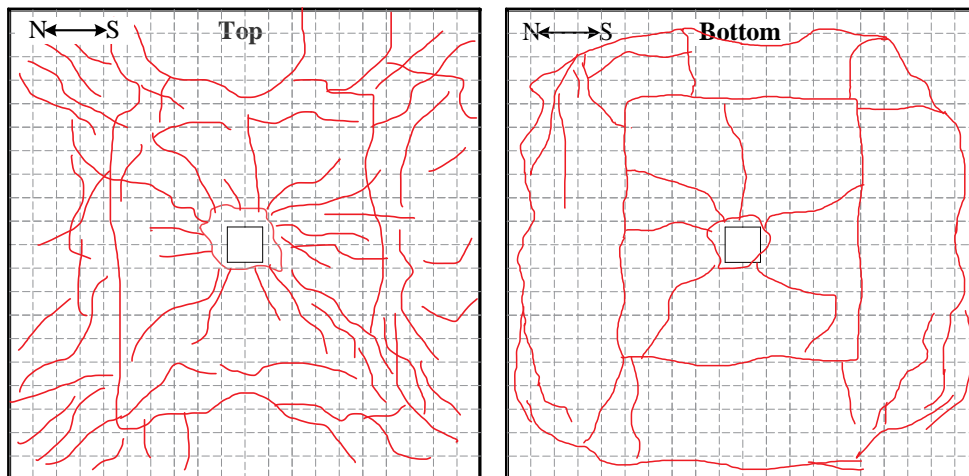
294



295

296

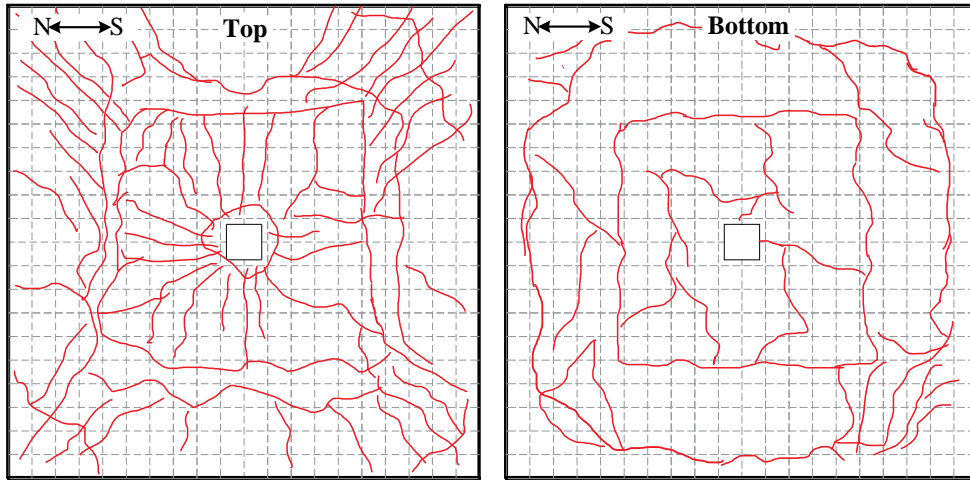
(a) DP



297

298

(b) SSR



299

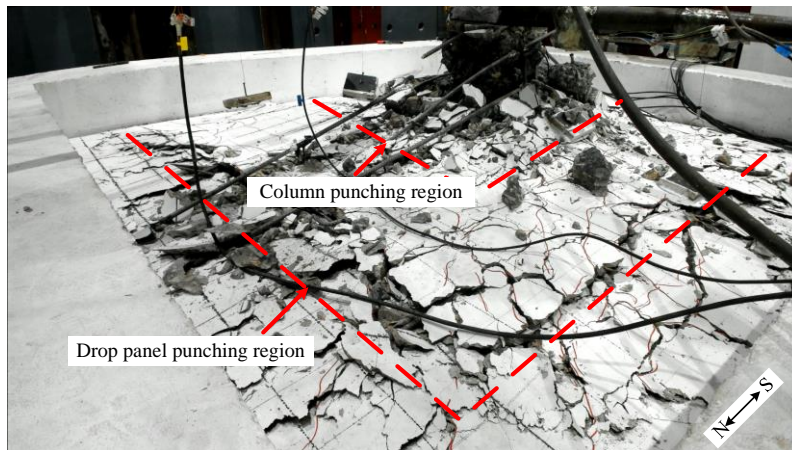
300

(c) SSO

301

Fig. 6. Crack patterns for DP, SSR and SSO.

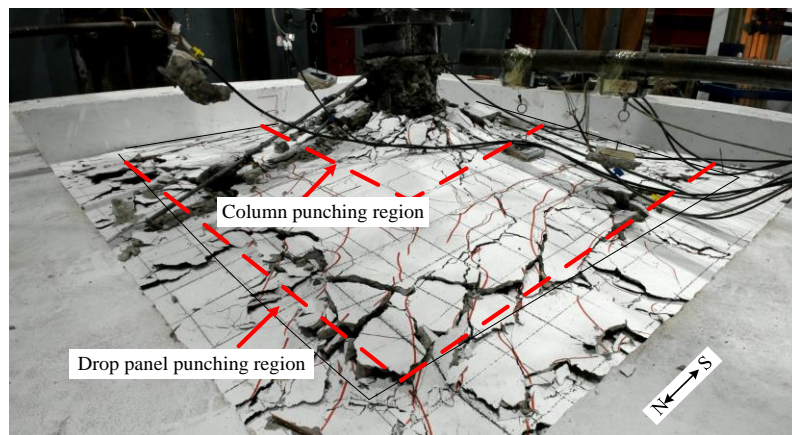
302



303

304

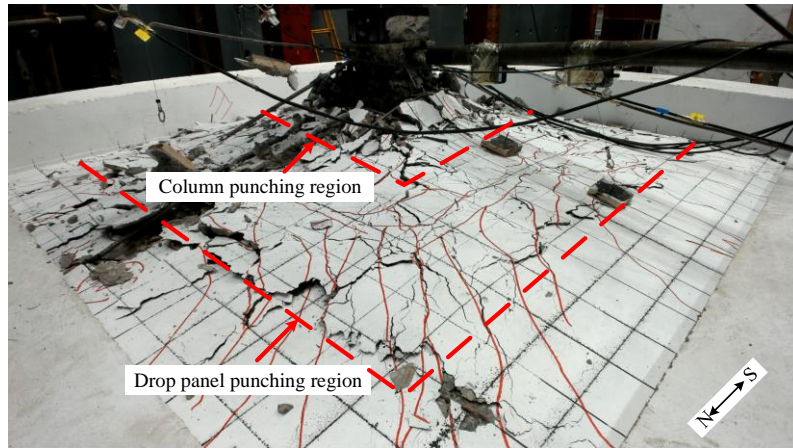
(a) DP



305

306

(b) SSR



(c) SSO

Fig. 7. The final failure modes on the slab top for DP, SSR and SSO.

307

308

309

310

311 The strain growth patterns of the through-column rebars (rebars A<sub>2</sub>, C and G) and non-through-

312 column rebars (rebars E, F and H) at positions close to the column perimeter region or the slab-

313 drop panel interface region are shown in Fig. 8. In the flexural stage before  $\Delta_{p1}$ , the strain near

314 the slab-drop panel interface region (i.e., ST<sub>2</sub>, SB<sub>2</sub>, ST<sub>4</sub>, SB<sub>4</sub>) increased faster than those near

315 the column perimeter region, indicating a relatively higher stress concentration at the slab-drop

316 panel interface where the first punching failure occurred. In general, FRs were in tension and

317 IRs were in compression. After the first punching failure, strains in IRs changed to tension,

318 reflecting that the load-resisting mechanism had transformed from the flexural mechanism to

319 the suspension mechanism. In the suspension stage I, fast strain growth was recorded in the

320 vicinity of the column perimeter region (i.e., ST<sub>1</sub>, SB<sub>1</sub>, ST<sub>3</sub>, SB<sub>3</sub>), as a result of stress

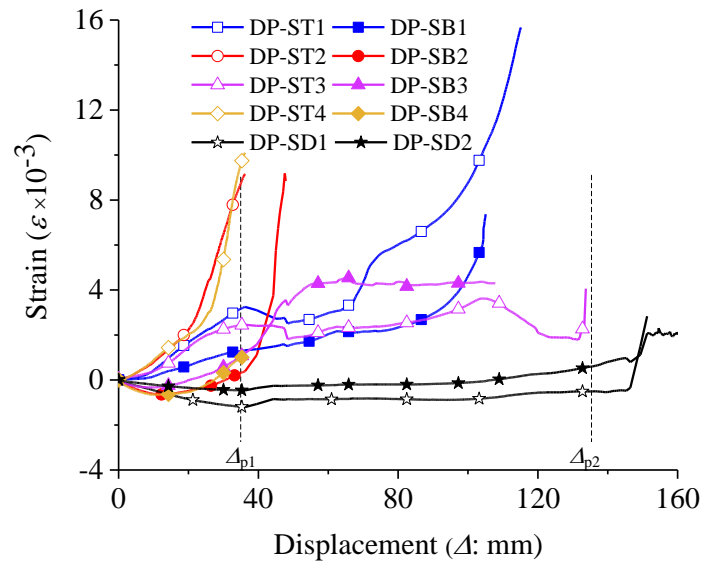
321 concentration moving from the slab-drop panel interface region to the column perimeter region.

322 Strains in the through-column rebar G and the non-through column rebar H within the drop

323 panel (i.e., SD<sub>1</sub> and SD<sub>2</sub>, respectively) remained in compression until the second punching

324 failure occurred, then started to transform into tension and grow further. The level of strain

325 growth in SD2 only slightly smaller than that in SD1, and both experienced rather small  
 326 variations. This indicates that the slab resisted the load as an integrated element with only a  
 327 small stress concentration along the orthogonal directions crossing the column.  
 328



329  
 330 Fig. 8. Rebar strain growth in DP.

331  
 332 **3.2 Specimens SSR and SSO**

333 Based on the test results, three major influences of the shear studs in SSR and SSO on the  
 334 mechanical behaviour of the two specimens are identified. Firstly, shear studs could provide  
 335 additional shear strength to resist the punching failure. Secondly, shear studs also offer  
 336 connections between the separated concrete on either side of the punching cracks, leading to  
 337 an improved integrity of the specimens. The second contribution is better reflected in the  
 338 ductility of the specimens when the second punching failure occurred. Thirdly, the inclusion of  
 339 shear studs, however, increased local stress concentration in the surrounding concrete, causing  
 340 inconsistent deformation between the concrete and shear studs. The interaction of these three

341 influences renders the mechanical behaviour of SSR and SSO more complicated.  
342  
343 Specifically, in the flexural stage, both SSR and SSO developed, on the slab top surface,  
344 diagonal cracks at the slab corners and the first square-shaped crack rings along the slab-drop  
345 panel interface at displacements  $\Delta=7\text{mm}$  and  $8\text{mm}$ , respectively (Figs. 5 and 6). The second  
346 crack rings at the onset of the first punching failure formed at  $\Delta=21\text{mm}$  and  $20\text{mm}$  for SSR  
347 and SSO, respectively (Figs. 5 and 6). The size of the second crack rings in SSR and SSO was  
348 almost the same as that in DP. In addition, the punching cracks in SSR and SSO developed  
349 earlier than those in DP. This is because a high level of stress concentration existed in the  
350 concrete surrounding the shear studs. Due to the additional shear resistance given by the shear  
351 studs, SSR and SSO demonstrated higher punching strengths, i.e.,  $F_{p1}=425\text{kN}$  and  $465\text{kN}$ ,  
352 which were 2.4% and 12% higher than that in DP, respectively. Shear studs also served as an  
353 ALP after the concrete has cracked, as reflected by the residual strengths  $F_{t1}$  after the first  
354 punching failure. The values of  $F_{t1}$  in SSR and SSO were  $283\text{kN}$  and  $281\text{kN}$ , respectively,  
355 which were on average 28.8% higher than that in DP.

356  
357 Shear studs were not as effective in improving the post-punching strength of the specimens.  
358 The post-punching strengths for SSR and SSO were  $F_{p2}=315\text{kN}$  and  $319\text{kN}$ , respectively,  
359 which were only increased by 1.6% and 2.9% as compared to DP. This is because the vertical  
360 shear studs were ineffective in transferring the load in the large deformation stage. Instead, the  
361 post-punching strengths were primarily governed by the rebars passing through the columns  
362 and other rebars crossing the punching cracks around the slab-drop panel interface. Shear studs

363 were also able to improve the integrity of the specimens and enhance the confinement effect  
364 for concrete. Hence, the second punching failure around the column perimeter in SSR and SSO  
365 exhibited a more ductile manner, and milder damages of SSR and SSO were observed  
366 compared to DP (Fig. 7). Moreover, the residual strengths  $F_{12}$  after the second punching failure  
367 were 275kN and 251kN for SSR and SSO, respectively, the drops in load resistance were only  
368 32.2% and 54.8% of that in DP. Both SSR and SSO specimens displayed a similar phenomenon  
369 in the final loading stage. With the pull-out and rupture of through-column rebars and bending  
370 of shear studs, the specimens eventually failed. The typical test phenomena with their  
371 corresponding  $F_s$  and  $\Delta s$  are also summarised in Table 3.

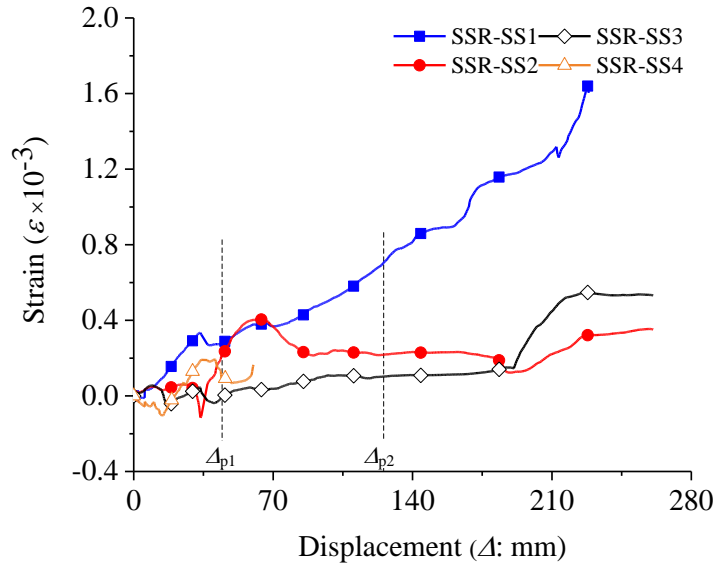
372

### 373 **3.3 Shear studs in radial and orthogonal patterns**

374 Adding shear studs contributed to improve the punching strengths  $F_{p1}$  of the slab-column joints  
375 with drop panels, and it was found that the shear studs in the orthogonal pattern performed  
376 better than those in the radial pattern. Radial arrangement (SSR) was insignificant in improving  
377  $F_{p1}$  (i.e., a 2.4% increase in  $F_{p1}$  comparing to DP), whereas a 12% increase in  $F_{p1}$  was found in  
378 the orthogonal arrangement (SSO). In SSO, the internal force transfer along the shortest  
379 orthogonal directions (Fig. 3(b)) was more prominent, due to comparatively more shear studs  
380 placed in these directions (compared to those in SSR) being able to better resist the shear forces  
381 together with concrete and the slab rebars FRs and IRs. This makes SSO more effective in  
382 resisting the first punching shear failure than SSR in which the shear studs were more evenly  
383 spread in radial directions. To further confirm this finding, Fig. 9(a) shows the strain growth  
384 pattern of the shear studs in SSR. It can be seen that the shear studs in the orthogonal directions

385 developed higher strains compared with those in the diagonal directions. Therefore, for the  
 386 same amount of shear studs, installing them all in the orthogonal directions would be more  
 387 effective in resisting the first punching failure.

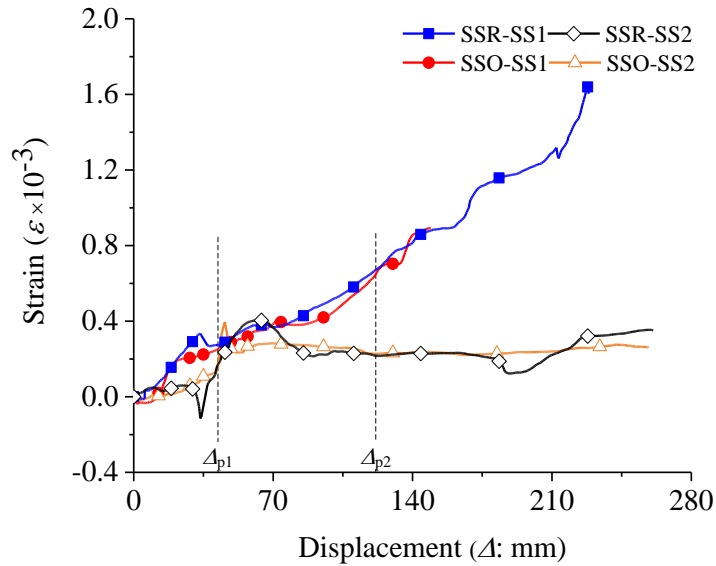
388



389

390

(a) Comparison between radial and orthogonal directions in SSR



391

392

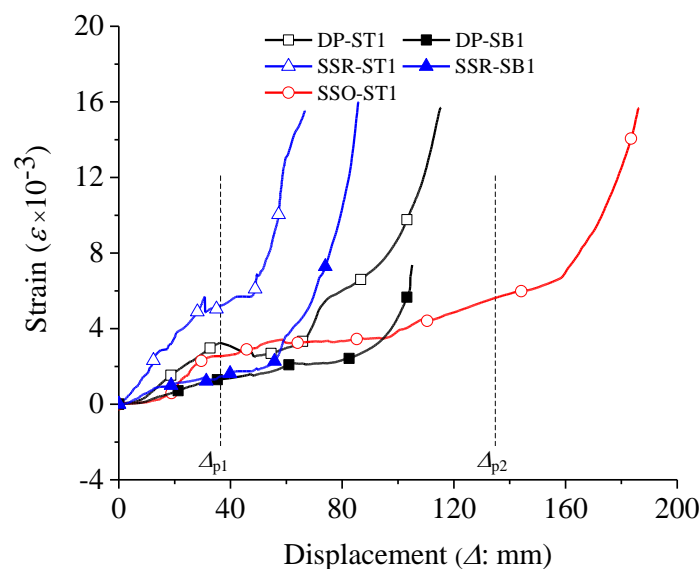
(b) Comparison between column perimeter and slab-drop panel interface regions

393

Fig. 9. Shear stud strain comparisons of SSR and SSO.

394

395 It is worthwhile noting that the shear studs inevitably induced local stress concentration. For  
 396 SSR, local stress concentration not only caused an earlier formation of punching cracks  
 397 comparing to DP, but also resulted in a sharp increase in rebar strain growth in the slab-drop  
 398 panel interface (Fig. 10), eventually leading to a premature punching failure ( $\Delta_{p1}=32\text{mm}$ ) and  
 399 a smaller punching strength enhancement ( $F_{p1}=425\text{kN}$ , a 2.4% increase from DP). For SSO,  
 400 the shear studs were placed in a double-row manner. The influence of local stress concentration  
 401 was offset by the additional shear resistance provided by the comparatively more shear studs  
 402 in the orthogonal directions than those in SSR. Therefore, the shear forces were more  
 403 effectively resisted by the shear studs in SSO than in SSR. Although the punching cracks in  
 404 SSO still formed earlier than DP, the rebar strains grew slower than those in DP and SSR (Fig.  
 405 10). The first punching failure was postponed and SSO was able to develop a higher punching  
 406 shear strength ( $F_{p1}=465\text{kN}$ , a 12% increase from DP). It is observed from Fig. 7 that damage  
 407 of SSO was less severe at the first punching failure (slab-drop panel interface) than DP and  
 408 SSR.



409  
 410 Fig. 10. Rebar strain comparisons of DP, SSR and SSO in slab-drop panel interface regions.

411

412 Adding shear studs helped to transfer the internal stresses in the concrete on both sides of the  
413 punching cracks, in turn improving the ductility around the column perimeter at the second  
414 punching failure. As such, the load drops of  $F_{t2}$  are more gradual in SSR and SSO, instead of  
415 being abrupt ( $F_{t1}$ ) in the first punching failure around the slab-drop panel interface (Fig. 5).  
416 This is because the cross-sectional area of punching around the slab-drop panel interface is far  
417 bigger than that around the column perimeter, therefore placing 8 rows of shear studs had a  
418 relatively minor contribution to the first punching failure of the entire slab-column joints.  
419 Referring to Fig. 5 again, shear studs in the radial pattern performed better in improving the  
420 residual strength  $F_{t2}$  after the second punching failure. Compared with SSO, SSR exhibited a  
421 lower load reduction and a relatively smoother damage process after the second punching  
422 failure. This is because the orthogonal directions of SSR had been severely damaged after the  
423 first punching failure. As a result, the shear studs positioned along the orthogonal directions  
424 lost much of their abilities to further strengthen the specimen. Nevertheless, apart from the  
425 orthogonal directions, shear studs were also arranged in the diagonal directions in SSR, which  
426 could play a major role in improving  $F_{t2}$  after the second punching failure. This finding can be  
427 supported by the strain growth patterns for the shear studs in Fig. 9(b). Strains near the column  
428 perimeter regions are higher than those near the slab-drop panel interface regions, suggesting  
429 that the shear studs had a higher level of influence on the column perimeter regions.

430

#### 431 **4. Validation of measured punching shear strengths against design codes**

432 Two different prediction methods for shear strengths of two-way slabs specified by ACI 318

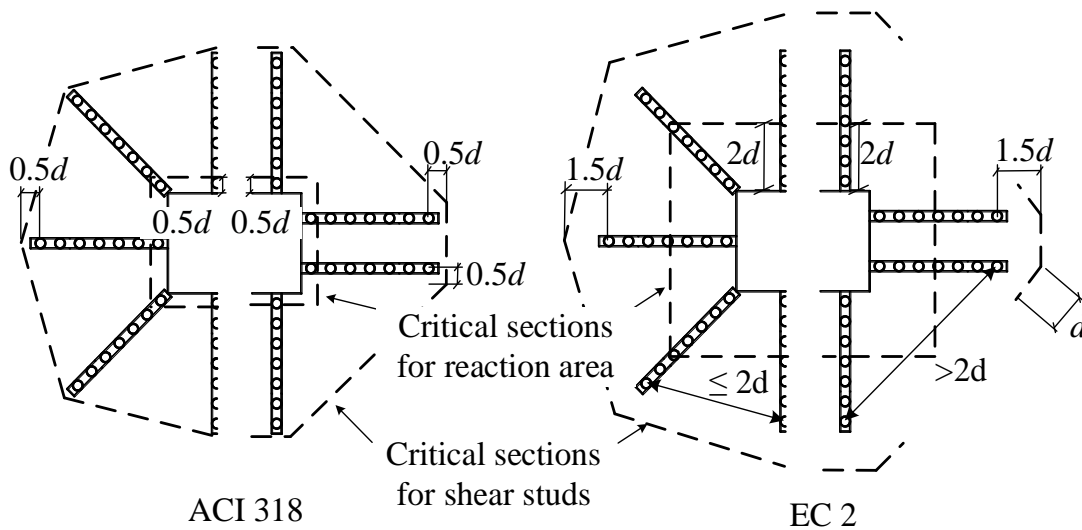
433 [24] and EC 2 [25] are also applicable for calculating the punching shear capacities of the three  
434 joint specimens in this study. Both design standards indicate that the punching shear strengths  
435 should be determined at the identified critical punching sections. Their provisions of  
436 identifying the critical sections and calculating the shear strengths are discussed herein, based  
437 on which the punching shear strengths of the three specimens are estimated and compared with  
438 the test results.

439

#### 440 **4.1 Critical sections**

441 The critical punching sections are considered as the sections where punching failure is likely  
442 to occur. There may exist multiple critical sections in a single slab-column joint and the shear  
443 strengths in these sections should be calculated separately. A punching failure was predicted to  
444 occur near the critical section when the minimum calculated strength was reached. Critical  
445 sections are assumed to be 45 degrees to the middle plane of the slab in ACI 318, whereas this  
446 angle is taken as 26.6 degrees in EC 2. To simplify the calculation, the critical sections are  
447 idealised to be perpendicular to the middle plane of the slab. ACI 318 requires that for slab-  
448 column joints without shear reinforcement, the critical sections should be located at a distance  
449  $d/2$  ( $d$  is the average effective depth in two orthogonal directions) from the face of the column.  
450 If the slab thickness varies, the critical sections should be determined at a distance  $d/2$  from  
451 where the slab thickness changes. For slab-column joints with shear reinforcement, in addition  
452 to the two critical sections defined above, another critical section is found at  $d/2$  beyond the  
453 outermost peripheral line of the shear reinforcement. Critical sections are also defined at a  
454 distance  $d/2$  beyond any point where variations in shear reinforcement occur (for example,

455 spacing). To reduce the perimeter ( $b_o$ ) of the critical sections beyond the outermost peripheral  
 456 line of shear reinforcement, the critical sections are set as a closed-polygon shape. The critical  
 457 section identification in ACI 318 is shown in Fig. 11. When designing the test specimens, two  
 458 critical sections were considered for DP and four critical sections, for SSR and SSO (Fig. 12).  
 459

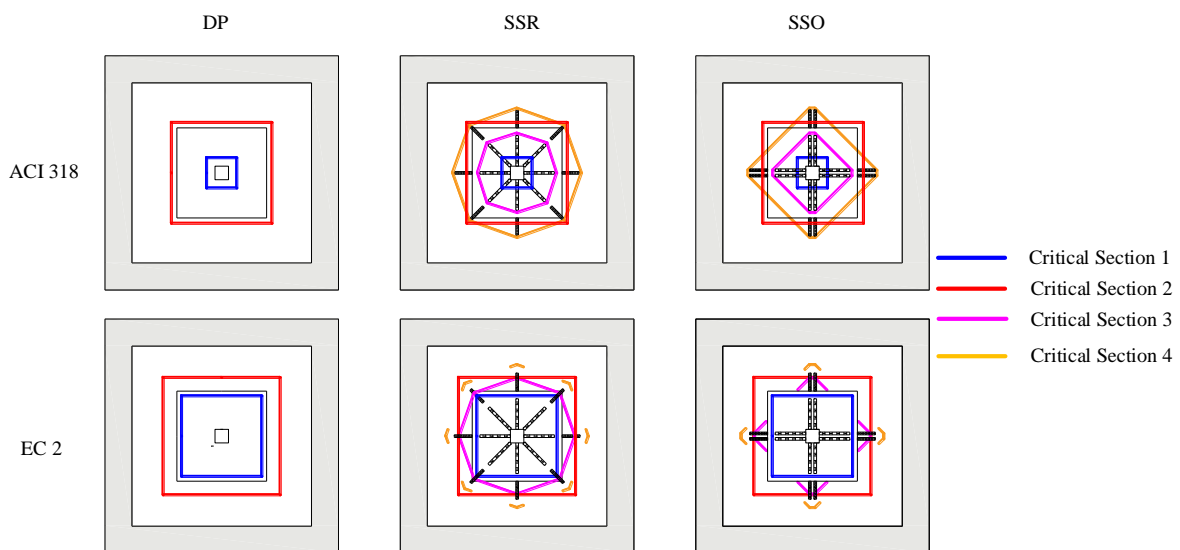


460

461

Fig.11. Critical section identifications in ACI 318 and EC 2.

462



463

464

Fig. 12. Critical sections in DP SSR and SSO.

465 In EC 2, for slab-column joints without shear reinforcement, the critical section is identified to

466 be located at  $2d$  from the column face and from where the slab thickness changes. For  
467 specimens with shear reinforcement, the critical section is also defined at  $1.5d$  from the  
468 discontinued position of the shear reinforcement. If the shear reinforcement varies in spacing,  
469 the critical section should be determined separately. In ACI 318, the critical section at the  
470 outermost periphery line of the shear studs is a closed polygon regardless of the shear stud  
471 arrangement, but this is not the case in EC 2, as shown in Fig. 11. It should be noted that  
472 although the shear studs were arranged in the radial pattern in the SSR specimen, the  
473 identification of the critical sections for the outermost periphery line of the shear studs in the  
474 slab-drop panel interface region follows a similar pattern as SSO. This is because the distance  
475 between the outermost shear studs in two adjacent rows is much greater than  $2d$ . The critical  
476 sections identification for the three specimens based on the rules in EC 2 is also illustrated in  
477 Fig. 12.

478

#### 479 **4.2 Prediction formulas**

480 The prediction formulas given in the two building codes are based on the same theoretical  
481 framework. For slab-column joints without shear reinforcement, the shear stress in the critical  
482 section is contributed by the concrete ( $v_c$ ) only. For slab-column joints with shear reinforcement,  
483 the shear stress is contributed by both the concrete ( $v_c$ ) and the shear reinforcement ( $v_s$ ). Note  
484 that all the formulas are given in SI units.

485

486 Considering the size effect, concrete properties and column location, the formula used to  
487 calculate  $v_{ACI318\ c}$  for slab-column joints without shear reinforcement is given in Eq. 1.

$$v_c^{\text{ACI318}} = \text{the least of} \begin{cases} 0.33\lambda_s^{\text{ACI318}}\lambda\sqrt{f'_c} \\ 0.17\left(1+\frac{2}{\beta}\right)\lambda_s^{\text{ACI318}}\lambda\sqrt{f'_c} \\ 0.083\left(2+\frac{asd}{b_o}\right)\lambda_s^{\text{ACI318}}\lambda\sqrt{f'_c} \end{cases} \quad (1)$$

488 where  $f'_c$  is the cylinder compressive strength of concrete (MPa);  $\lambda_s^{\text{ACI318}}$  is the size effect  
 489 factors,  $\lambda_s^{\text{ACI318}} = (2/(1+0.004d))^{0.5} \leq 1$ ;  $\lambda$  is the modification factor reflecting the reduced  
 490 mechanical properties of lightweight concrete, for normal strength concrete,  $\lambda=1$ ;  $\beta$  is the  
 491 aspect ratio of the column cross section, or the reaction area;  $\alpha_s$  is the column location factor,  
 492 taken as 40 for interior column.

493

494 For slab-column joints with shear reinforcement, the contribution of the concrete to the shear  
 495 stress at the critical sections is reduced, which can be calculated by Eq. 2.

$$v_c^{\text{ACI318}} = \text{the least of} \begin{cases} 0.25\lambda_s^{\text{ACI318}}\lambda\sqrt{f'_c} \\ 0.17\left(1+\frac{2}{\beta}\right)\lambda_s^{\text{ACI318}}\lambda\sqrt{f'_c} \\ 0.083\left(2+\frac{asd}{b_o}\right)\lambda_s^{\text{ACI318}}\lambda\sqrt{f'_c} \end{cases} \quad (2)$$

496

497 Shear stress contributed by the concrete in the critical sections at the outermost of shear studs  
 498 can be calculated using Eq. 3.

$$v_c^{\text{ACI318}} = 0.17\lambda_s^{\text{ACI318}}\lambda\sqrt{f'_c} \quad (3)$$

499 Shear stress contributed by the shear studs can be estimated by Eq. 4

$$v_s^{\text{ACI318}} = \frac{A_v f_{yt}}{b_o s} \quad (4)$$

500 where  $A_v$  is the sum of the area of all legs of shear studs on one peripheral line that is

501 geometrically similar to the perimeter of the column section;  $f_{yt}$  is the yield strength of the shear  
502 studs;  $s$  is the spacing of the shear studs.

503

504 EC 2 considers the influence of the tensile reinforcement ratio in addition to the size effect and  
505 the concrete strength when calculating the shear stress contributed by the concrete, as expressed  
506 in Eq. 5

$$v_c^{EC2} = 0.12\lambda_s^{EC2}(100\rho_1f_c')^{1/3} \quad (5)$$

507 where  $\lambda_s^{EC2}$  is the size effect factor;  $\lambda_s^{EC2} = 1 + (200/d)^{0.5} \leq 2$ ;  $\rho_1$  is the parameter related to the  
508 tensile reinforcement ratio,  $\rho_1 = (\rho_{ly} \times \rho_{lz})^{0.5} \leq 0.02$  in which  $\rho_{ly}$  and  $\rho_{lz}$  are the bonded tension  
509 reinforcement ratios in two orthogonal directions within the reaction area plus a  $3d$  extension.

510

511 EC2 specifies that the concrete contribution to the shear stress is only 75% effective if shear  
512 reinforcement exists. Shear stress contributed by the shear reinforcement is calculated based  
513 on Eq. 6.

$$v_s^{EC2} = 1.5(d/s)A_v f_{yt,ef} (1/b_o d) \sin \alpha \quad (6)$$

514 where  $f_{yt,ef}$  is the effective yield strength of the shear reinforcement,  $f_{yt,ef} = 250 + 0.25d \leq f_{yt}$ ;  $\alpha$  is  
515 the angle between the shear reinforcement and the mid-plane of the slab.

516

### 517 **4.3 Compression between code predictions and test results**

518 The results of the theoretical calculations based on the two building codes are presented in  
519 Table 4. The shear strength reduction factors were not considered in calculations as the

520 predictions were compared to the ultimate capacities of the specimens in the tests. The code  
521 predictions for the punching failure locations are aligned with the experimental observations.  
522 For the specimen without shear studs (DP), the punching shear strength predictions by both  
523 codes were conservative. This was safe in design, however, the material strengths may not be  
524 fully utilised. For the specimens with shear studs (SSR and SSO), both codes overestimate the  
525 punching strengths. The results predicted by ACI 318 had higher discrepancies than EC 2 with  
526 reference to the test results. This is due to the assumption in ACI 318 that the shear strength  
527 provided by the shear studs could reinforce the concrete area in a uniform manner, regardless  
528 of their arrangement. In reality, if the two adjacent rows of shear studs are far apart, the concrete  
529 between them could not be effectively strengthened. EC 2, on the other hand, considers the  
530 influence caused by uneven strengthening. When defining the outermost critical sections, if the  
531 distance between the two adjacent rows of shear studs was too large, only a part of the area was  
532 selected as shown in Fig. 11 and Fig. 12. Nonetheless, the results predicted by EC 2 are still  
533 higher than the experimental values. Furthermore, complicated mechanical behaviour in slab-  
534 column joints with drop panels and shear studs may lead to premature punching failure, like in  
535 the case of SSR, which was not considered in the code predictions. More experimental tests  
536 would be required to further investigate the performance of the design codes in predicting the  
537 punching shear strengths, so as to offer more conclusive recommendations. Moreover, post-  
538 punching strengths cannot be predicted theoretically, as the post-punching load-resistant  
539 mechanisms are not considered in the codes.

540

541

542

Table 4. Punching shear strength comparison between code predictions and results

Specimen	Code	Critical section				$V_{p,cal}$ (kN)	$V_{p,exp}$ (kN)	$V_{p,cal}/$ $V_{p,exp}$
		Section 1 (kN)	Section 2 (kN)	Section 3 (kN)	Section 4 (kN)			
DP	ACI 318	421	375	N/A	N/A	415	375	0.90
	EC 2	292	216	N/A	N/A		216	0.52
SSR	ACI 318	643	735	1076	649	425	643	1.51
	EC 2	691	677	720	522		522	1.23
SSO	ACI 318	643	735	1042	625	465	625	1.34
	EC 2	691	677	577	540		540	1.16

543 Note:  $V_{p,cal}$  and  $V_{p,exp}$  represent the calculated and tested punching shear strength, respectively.

544

## 545 5. Conclusions

546 Quasi-static tests on three slab–column joint specimens with drop panels, and with and without  
547 shear studs were conducted and reported. The specimens were subjected to appropriate in-plane  
548 restraints and were tested until large deformation stages under a monotonic upward loading.  
549 Punching shear strengths of the three specimens were also predicted theoretically the two  
550 building codes. Based on the experimental and theoretical results, the following conclusions  
551 can be drawn.

552

553 1. For all three specimens, two punching failures was observed at the slab-drop panel  
554 interface regions and the column perimeter regions during the entire deformation stages.

555 Before the first punching failure, the load was resisted mainly by the flexural mechanism.

556 Yet, the post-punching resistance were provided and governed by the rebars going through  
557 the columns and the others crossing the punching cracks.

558 2. Adding shear studs can improve resistance to punching shear failure. Compared to DP,  
559 SSR and SSO had a 2.4% and 12% increase in punching strengths, respectively. However,  
560 using shear studs were not as efficient in improving the post-punching strengths, as SSR  
561 and SSO had only 1.6% and 2.9% increase, respectively. Nevertheless, shear studs could  
562 help to improve the ductility of the joints, thus the second punching failure exhibited a  
563 more ductile manner and the residual strengths after the second punching failure were also  
564 improved in both SSR and SSO.

565 3. Shear studs may lead to a higher stress concentration in the orthogonal directions crossing  
566 the column than the diagonal directions, resulting in a rapid growth in the reinforcement  
567 strain. This mechanical behaviour affected further development of the punching strength  
568 in SSR, leading to a premature punching shear failure. Such an unfavourable effect was  
569 neutralised in the specimen SSO due to comparatively more shear studs being placed in  
570 the orthogonal directions than in SSR to resist shear. Shear studs in the orthogonal pattern  
571 were found to be more effective in enhancing punching strength. After the first punching  
572 failure in all specimens, damage along the orthogonal directions was observed to be more  
573 severe than the diagonal directions. In SSR in particular, the capacity in resisting the shear  
574 has lost much on the orthogonally placed shear studs whereas diagonally arranged shear  
575 studs were still able to resist the load. As a result, shear studs in the radial pattern are more  
576 beneficial in mitigating the second punching failure around the column perimeter region.

577 4. Theoretical calculations based on ACI 318 and EC 2 underestimate the punching shear

578 strength of DP but overestimate those of SSR and SSO. Further experimental and  
579 theoretical investigations are necessary to establish a more accurate calculation method for  
580 slab-column joints with drop panels and shear studs.

581

## 582 **Acknowledgement**

583 The authors are grateful for the financial support received from the National Natural Science  
584 Foundation of China (No. 52178094), the National Key Research and Development Program  
585 of China (No. 2019YFC1511000), the 111 Project (No. D21001), and the Australian Research  
586 Council through an ARC Discovery Project (DP150100606).

587

## 588 **References**

- 589 [1] R. Park, W.L. Gamble, Reinforced concrete slabs, John Wiley & Sons, 1999.
- 590 [2] ASCE/SEI 7–16. Minimum Design Loads and Associated Criteria for Buildings and Other  
591 Structures, American Society of Civil Engineers, Virginia, USA, 2017.
- 592 [3] N.J. Gardner, J. Huh, L. Chung, Lessons from the Sampoong department store collapse,  
593 Cem. Concr. Compos. 24 (6) (2002) 523-529.
- 594 [4] X.Z. Lu, H. Guan, H.L. Sun, Y. Li, Z. Zheng, Y.F. Fei, Z. Yang, L.X. Zuo, A preliminary  
595 analysis and discussion of the condominium building collapse in surfside, Florida, US, June  
596 24, 2021, Front. Struct. Civ. Eng. 15 (5) (2021) 1097-1110.
- 597 [5] Department of Defense (DoD). Unified Facilities Criteria (UFC): Design of Structures to  
598 Resist Progressive Collapse, Washington D.C., USA, 2016.
- 599 [6] General Service Administration (GSA). Progressive Collapse Analysis and Design  
600 Guidelines for New Federal Office Buildings and Major Modernization Projects, Washington  
601 D.C., USA, 2016.

- 602 [7] N.M. Hawkins, D. Mitchell, Progressive collapse of flat plate structures, *ACI J.* 76 (7) (1979)  
603 775-808.
- 604 [8] Y. Tian, J.O. Jirsa, O. Bayrak, Widiyanto, J.F. Argudo, Behavior of slab-column connections  
605 of existing flat-plate structures, *ACI Struct. J.* 105 (5) (2008) 561-569.
- 606 [9] A. Muttoni, Punching shear strength of reinforced concrete slabs without transverse  
607 reinforcement, *ACI Struct. J.* 105 (4) (2008) 440-450.
- 608 [10] S. Guandalini, O.L. Burdet, and A Muttoni, Punching tests of slabs with low reinforcement  
609 ratios, *ACI Struct. J.* 106 (1) (2009) 87-95.
- 610 [11] M.Z. Diao, Y. Li, H. Guan, Z. Yang, B.P. Gilbert, J.K. Wang, Pre- and post-punching  
611 performances of eccentrically loaded slab-column joints with in-plane restraints, *Eng. Struct.*  
612 248 (2021) 113249.
- 613 [12] M.Z. Diao, Y. Li, H. Guan, X.Z. Lu, H.Z. Xue, Z.D. Hao, Post-punching mechanisms of  
614 slab-column joints under upward and downward punching actions, *Mag. Concr. Res.* 73 (6)  
615 (2021) 302-314.
- 616 [13] Y.Z. Yang, Y. Li, H. Guan, M.Z. Diao, X.Z. Lu, Enhancing post-punching performance  
617 of flat plate-column joints by different reinforcement configurations, *J. Build. Eng.* 43 (2021)  
618 102855.
- 619 [14] M. F. Ruiz, Y. Mirzaei, A. Muttoni, Post-punching behavior of flat slabs, *ACI Struct. J.*  
620 110 (5) (2013) 801-812.
- 621 [15] A.L. Carvalho, G.S. Melo, R.B. Gomes, P.E. Regan, Punching shear in post-tensioned flat  
622 slabs with stud rail shear reinforcement, *ACI Struct. J.* 108 (5) (2011) 523-531.
- 623 [16] W.J. Yi, F.Z. Zhang, S.K. Kunnath, Progressive collapse performance of RC flat plate  
624 frame structures, *J. Struct. Eng.* 140 (9) (2014) 04014048.
- 625 [17] W. Salim, W.M. Sebastian, Punching shear failure in reinforced concrete slabs with  
626 compressive membrane action, *ACI Struct. J.* 100 (4) (2003) 471-479.

627 [18] L. Keyvani, M. Sasani, Y. Mirzaei, Compressive membrane action in progressive collapse  
628 resistance of RC flat plates, *Eng. Struct.* 59 (2014) 554-564.

629 [19] Z.H. Peng, S.L. Orton, J.R. Liu, Y. Tian, Effects of in-plane restraint on progression of  
630 collapse in flat-plate structures, *J. Perform. Constr. Facil.* 31 (3) (2017) 04016112.

631 [20] P.X. Dat, T.K. Hai, Membrane actions of RC slabs in mitigating progressive collapse of  
632 building structures, *Eng. Struct.* 55 (2013) 107-115.

633 [21] X.G. Wu, S.Y. Yu, S.C. Xue, T.H.K. Kang, H.J. Hwang, Punching shear strength of  
634 UHPFRC-RC composite flat plates, *Eng. Struct.* 184 (2019) 278-286.

635 [22] P. Zohrevand, X. Yang, X. Jiao, A. Mirmiran, Punching shear enhancement of flat slabs  
636 with partial use of ultrahigh-performance concrete, *J. Mater. Civ. Eng.* 27 (9) (2015) 04014255.

637 [23] L.N. Minh, M. Rovňák, T.T. Ngoc, T.L. Phuoc, Punching shear resistance of post-  
638 tensioned steel fiber reinforced concrete flat plates, *Eng. Struct.* 45 (2012) 324-337.

639 [24] ACI 318-19. Building Code Requirements for Structural Concrete and Commentary,  
640 American Concrete Institute, Detroit. USA, 2019.

641 [25] EN 1992-1-1:2004. Eurocode 2: Design of Concrete Structures-part 1-1: General Rules  
642 and Rules for Buildings, European Committee for Standardization, 2004.

643 [26] GB 50010-2010. Code for Design of Concrete Structures, China Architecture & Building  
644 Press, Beijing, China, 2015.

645 [27] K. Qian, B. Li, Experimental study of drop-panel effects on response of reinforced  
646 concrete flat slabs after loss of corner column, *ACI Struct. J.* 110 (2) (2013) 319-330.

647 [28] K. Qian, B. Li, Load-resisting mechanism to mitigate progressive collapse of flat slab  
648 structures, *Mag. Concr. Res.* 67 (7) (2015) 349-363.

649 [29] Y.H. Weng, K. Qian, F. Fu, Q. Fang, Numerical investigation on load redistribution  
650 capacity of flat slab substructures to resist progressive collapse, *J. Build. Eng.* 29 (2020)  
651 101109.

- 652 [30] K. Qian, Y.H. Weng, B. Li, Impact of two columns missing on dynamic response of RC  
653 flat slab structures, *Eng. Struct.* 177 (2018) 598-615.
- 654 [31] P.H. Langohr, A. Ghali, W.H. Dilger, Special shear reinforcement for concrete flat plates,  
655 *ACI J.* 1976, 73 (3) (1976) 141-146.
- 656 [32] F. Seible, A. Ghali, W.H. Dilger, Preassembled shear reinforcing units for flat plates, *ACI*  
657 *J.* 77 (1) (1980) 28-35.
- 658 [33] G. Birkle, W.H. Dilger, Shear strength of slabs with double-headed shear studs in radial  
659 and orthogonal layouts, *ACI Struct. J. Special Publication* 265 (2009) 499-510.
- 660 [34] C.E. Broms, Ductility of flat plates: comparison of shear reinforcement systems, *ACI*  
661 *Struct. J.* 104 (6) (2007) 703-711.
- 662 [35] T.X. Dam, J.K. Wight, Flexurally-triggered punching shear failure of reinforced concrete  
663 slab-column connections reinforced with headed shear studs arranged in orthogonal and radial  
664 layouts, *Eng. Struct.* 110 (2016) 258-268.
- 665 [36] JGJ 92-2016. Technical specification for concrete structures prestressed with unbonded  
666 tendons, China Architecture & Building Press, Beijing, China, 2016.